Asymptotics in Curve Estimation Based on Partial Fitting with Piecewise Bézier Cubics

Ryszard Kozera[1,2,3][0000−0002−2907−8632] and Magdalena Wilkołazka[2][0000−0003−4056−5922]

[1] Warsaw University of Life Sciences - SGGW
Institute of Information Technology
Ul. Nowoursynowska 166, 02-787 Warsaw, Poland
ryszard_kozera@sggw.pl
ryszard.kozera@gmail.com

[2] The John Paul II Catholic University of Lublin
Faculty of Social and Technical Sciences
Ul. Konstantynów 1H, 20-708 Lublin, Poland
magda.wilkolazka@gmail.com
magda8310@kul.lublin.pl

[3] The University of Western Australia
School of Physics, Mathematics and Computing
35 Stirling Highway, Crawley, 6009 WA, Perth, Australia
ryszard.kozera@uwa.edu.au

Abstract. The problem of fitting reduced data representing the sequence of interpolation points of curve γ in arbitrary Euclidean space is examined here. In our setting, the corresponding interpolation knots are assumed to be unknown. In this work the so-called piecewise Bézier cubic fitting scheme $\hat{\gamma}$ is applied to partially interpolate reduced data based on local replacement of the unknown knots. In exchange for partial interpolation, the fitting scheme in question preserves all geometrical properties ingrained by Bézier cubic curves (designed mainly for modelling purposes). The main theoretical contribution of this work establishes linear, quadratic or in-between sharp asymptotics in estimating γ by $\hat{\gamma}$, subject to the character of various admissible samplings. The convergence orders proved in this work are ultimately verified numerically in affirmative as sharp. The tests are conducted on 2D and 3D curves with the aid of *Mathematica software package*. Finally, potential extensions and some applications of this work are briefly outlined.

Keywords: Interpolation and Reduced Data · Convergence Orders and Sharpness · Bézier Curves · Computer Graphics and Modelling.

1 Introduction

We analyze the problem of interpolating reduced data $Q_n = \{q_0, q_1, \dots, q_n\}$ in arbitrary Euclidean space $\mathbb{E}^m$. It is assumed here that for some C^2 class parametric curve $\gamma : [0, T] \to \mathbb{E}^m$ (see e.g. [5, 15]) satisfying $q_i = \gamma(t_i)$ the

ICCS Camera Ready Version 2026
To cite this paper please use the final published version:
DOI: 10.1007/978-3-032-29909-3_25

corresponding interpolation knots $\mathcal{T}_n = \{t_i\}_{i=0}^n$ (subject to $t_i < t_{i+1}$) remain unknown. In order to fit Q_n (called reduced data) with any interpolation scheme the unknown knots $\mathcal{T}_n$ need to be somehow compensated with some substitutes $\hat{\mathcal{T}}_n = \{\hat{t}_i\}_{i=0}^n$ set in ascending order (see [4, 29]). Various interpolation schemes $\hat{\gamma}$ based on different knots recipes are studied e.g. in [2, 4, 6, 10, 24, 35, 38] (for dense Q_n) or e.g. in [21–23, 28, 39] (for sparse Q_n). In case of dense reduced data Q_n the issue of convergence rate in approximating γ by a given $\hat{\gamma}$ and $\hat{\mathcal{T}}_n$ is examined e.g. in [7, 10, 11, 20, 24–27]. In general, any convergence established does not enforce in principle extra geometrical properties possibly imposed on $\hat{\gamma}$ (e.g. the convexity of $\hat{\gamma}$ - see [36, 37]). The latter usually requires a careful treatment referring to a proper choice of fitting curve $\hat{\gamma}$ and the selection of the knots $\hat{\mathcal{T}}_n$.

In this work we analyze the problem of partially fitting Q_n by interpolating merely $Q_n^p = \{q_0, q_3, q_6, \ldots, q_{n-3}, q_n\} \subset Q_n$ (here $n = 3l$, where $l \in \mathbb{N}$) with the so-called piecewise Bézier cubic curve $\hat{\gamma}$ (see Section 3). The remaining interpolation points $Q_n \setminus Q_n^p = \{q_1, q_2, q_4, q_5, \ldots, q_{n-2}, q_{n-1}\}$ serve here only as control points - see e.g. [37]. Such approach permits the fitting curve $\hat{\gamma}$ to inherit all local geometrical features of Bézier cubic curves (see [37]; Section 1.3) and equally to preserve the approximation property by interpolating Q_n^p (representing less than half of all interpolation points Q_n).

The main theoretical contribution of this work (see Th. 1 and Ex. 1 in Section 5) establishes sharp asymptotics in γ estimation by piecewise Bézier cubic curve $\hat{\gamma}$ (see Section 3) sampled by various subfamilies of admissible samplings $\mathcal{T}_n$ (see Section 2). In particular, *linear, quadratic* or $\min\{2, 1+\varepsilon\}$ sharp orders are proved once γ is sampled *admissibly or more-or-less uniformly*, *uniformly* or *ε-uniformly* (see Section 2). Noticeably, though $\hat{\gamma}$ fits only $Q_n \setminus Q_n^p$ the proof of Th. 1 exploits full interpolation information encoded in Q_n upon resorting to all constraints $q_i = \gamma(t_i)$, with $i = 0, 1, 2, \ldots, n$. Finally, Section 6 verifies numerically in affirmative the asymptotics from Th. 1 with the aid of *Mathematica software package*. Though all numerical tests are conducted here only for 2D and 3D curves, they also apply to arbitrary m-dimensional curves. The paper completes with conclusions supplemented with some hints on possible applications and extensions of this work - see Section 7.

2 Admissible Samplings

In this section, basic notions on samplings $\mathcal{T}_n$ are recalled (see e.g. [17]).

Definition 1. *The corresponding tabular parameters $\mathcal{T}_n = \{t_i\}_{i=0}^n$ satisfy:*

$$\lim_{n\to\infty} \delta_n \to 0^+, \quad \text{where} \quad \delta_n = \max_{1\leq i\leq n} \{t_i - t_{i-1} : i = 1, 2, \ldots, n\}. \tag{1}$$

A special subfamily of admissible samplings (see e.g. [36]) called *more-or-less uniform* is introduced next.

ICCS Camera Ready Version 2026
To cite this paper please use the final published version:
DOI: 10.1007/978-3-032-29909-3_25

Definition 2. *The sampling* $\mathcal{T}_n = \{t_i\}_{i=0}^n$ *is more-or-less uniform if for some constants* $0 < K_l \leq K_u$ *and sufficiently large* n:

$$\frac{K_l}{n} \leq t_i - t_{i-1} \leq \frac{K_u}{n}, \tag{2}$$

for $i = 1, 2, \ldots, n$. *Condition* (2) *can be replaced by* $\beta\delta_n \leq t_{i+1} - t_i \leq \delta_n$ *satisfied for some* $0 < \beta \leq 1$ *and sufficiently large* n.

In particular if $K_l = K_u$ (which by $\sum_{i=0}^n (t_{i+1} - t_i) = T$ yields $K_l = K_u = T$) formula (2) represents *a uniform sampling*.

A small perturbation of uniform sampling is no longer uniform but may approach uniformity in the asymptotic sense. In particular, a special subfamily of admissible samplings called *ε-uniform samplings* is defined according to (see e.g. [17]):

Definition 3. *For* $\varepsilon > 0$, *the knots* $\mathcal{T}_n = \{t_i\}_{i=0}^n$ *are* ε*-uniformly sampled, if there exists an order preserving* $\phi : [0, T] \to [0, \hat{T}]$ *of class* C^2 *i.e.* $\dot{\phi} > 0$, *such that:*

$$t_i = \phi(\frac{iT}{n}) + O(\frac{1}{n^{1+\varepsilon}}). \tag{3}$$

Note that in Def. 3 the mapping ϕ is assumed to be at least of class C^2 as the second order Taylor expansion of ϕ is used to prove (9).

3 Piecewise Bézier cubic curve

The Bézier cubic curve $\hat{\gamma}_i : [0, 1] \to \mathbb{E}^m$ defined by four control points $\mathcal{Q}_i = \{q_i\}_{j=0}^{i+j}$ (for $j = 0, 1, 2, 3$ and $q_{i+j} \in \mathbb{E}^m$) is determined in the parametric form (see e.g. [37]) by the following formula (for $s \in [0, 1]$):

$$\hat{\gamma}_i(s) = \binom{3}{0}(1-s)^3 s^0 q_i + \binom{3}{1}(1-s)^2 s^1 q_{i+1} + \binom{3}{2}(1-s)^1 s^2 q_{i+2} + \binom{3}{3}(1-s)^0 s^3 q_{i+3}. \tag{4}$$

Each cubic $\hat{\gamma}_i$ interpolates two terminal points $\hat{\gamma}_i(0) = q_i$ and $\hat{\gamma}_i(1) = q_{i+3}$ with $\hat{\gamma}_i'(0)$ parallel to $q_{i+1} - q_i$ and $\hat{\gamma}_i'(1)$ parallel to $q_{i+3} - q_{i+2}$. The trajectory of $\hat{\gamma}_i$ is contained in the convex hull determined by $\mathcal{Q}_i$ enforcing extra geometrical properties on the piecewise Bézier cubic curve $\hat{\gamma}$ controlled by $\mathcal{Q}_0$, $\mathcal{Q}_3$, $\mathcal{Q}_6, \ldots$, $\mathcal{Q}_{n-3}$ with the aid of $\hat{\gamma}_0$, $\hat{\gamma}_3$, $\hat{\gamma}_6$, ..., $\hat{\gamma}_{n-3}$, respectively.

In order to compare both curves γ and $\hat{\gamma}$ their domains must be somehow related. In doing so, define a family of affine mappings $\psi_i : [t_i, t_{i+3}] \to [0, 1]$ determined by:

$$\psi_i(t) = \frac{t - t_i}{t_{i+3} - t_i}, \tag{5}$$

yielding

$$\dot{\psi}_i(t) = \frac{1}{t_{i+3} - t_i} \quad \textit{and} \quad \ddot{\psi}_i(t) = 0. \tag{6}$$

ICCS Camera Ready Version 2026
To cite this paper please use the final published version:
DOI: 10.1007/978-3-032-29909-3_25

From now on, let $\psi : [0,T] \to \mathbb{R}$ define a track-sum of $\{\psi_i\}_{i=0}^{n-1}$. At this point, it is worth re-emphasizing the most important geometrical properties of Bézier cubic curve $\hat{\gamma}_i$ based on four control points $\mathcal{Q}_i$ (see [37]; Section 1.3). Naturally, these features are locally preserved by a piecewise Bézier cubic curve $\hat{\gamma}$ based on Q_n^p. The overall property of $\mathcal{Q}_i$ "approximating the shape" of $\hat{\gamma}_i$ can be more precisely reformulated as:

- $\hat{\gamma}_i$ trajectory is contained in the convex hull defined by control points $\mathcal{Q}_i$;
- the interpolation conditions $\hat{\gamma}_i(0) = q_i$ and $\hat{\gamma}_i(1) = q_{i+3}$ hold;
- the endpoint tangent directions $\hat{\gamma}_i'(0)$ and $\hat{\gamma}_i'(1)$ are parallel to $q_{i+1} - q_i$ and $q_{i+3} - q_{i+2}$, respectively;
- the curve $\hat{\gamma}_i$ initially (at $s = \hat{t}_i = 0$) turns into a direction as $q_i q_{i+1} q_{i+2}$ and finally (at $s = \hat{t}_{i+3} = 1$) turns into direction $q_{i+1} q_{i+2} q_{i+3}$.

Observe that the mapping ψ_i transforms the subinterval $[t_i, t_{i+3}]$ into $[0,1]$ which forms the domain of each $\hat{\gamma}_i$ introduced in (4).

4 Convergence and Sharpness

Basic definitions and notions on convergence orders and their sharpness are given in this section (see e.g. [17]).

Definition 4. *Consider a family $\{f_{\delta_n}, \delta_n > 0\}$ of functions $f_{\delta_n} : I \to \mathbb{E}$. We say that f_{δ_n} is of order $O(\delta_n^\alpha)$ (denoted as $f_{\delta_n} = O(\delta_n^\alpha)$), if there is a constant $K > 0$ such that, for some $\bar{\delta} > 0$ the inequality $|f_{\delta_n}(t)| < K\delta_n^\alpha$ holds for all $\delta_n \in (0, \bar{\delta})$, uniformly over I. For the family of vector-valued functions $F_{\delta_n} : I \to \mathbb{E}^m$ by $F_{\delta_n} = O(\delta_n^\alpha)$ it is understood that $\|F_{\delta_n}\| = O(\delta_n^\alpha)$.*

Definition 5. *For a given scheme $\hat{\gamma}$ interpolating Q_n with some knots' estimates $\hat{\mathcal{T}} \approx \mathcal{T}$ (and some chosen mapping $\phi : I \to \hat{I}$) the asymptotics $\gamma - \hat{\gamma} \circ \phi = O(\delta_n^\alpha)$* is sharp *over I within the prescribed families of curves $\mathcal{J}$ and samplings $\mathcal{K}$, if there exist $\gamma \in \mathcal{J}$ and $\mathcal{T} \in \mathcal{K}$ such that for some $t^* \in I$ and some $K > 0$ we have $\|\gamma(t^*) - (\hat{\gamma} \circ \phi)(t^*)\| = K\delta_n^\alpha + O(\delta_n^\theta)$, where $\theta > \alpha$.*

Note that for an arbitrary more-or-less uniform sampling $\mathcal{T}_n$ any asymptotics $F_{\delta_n} = O(\delta_n^\alpha)$, by (1) and (2) results in $F_{\delta_n} = O(\frac{1}{n^\alpha})$.

In the next section we establish and prove the main result of this paper determining the asymptotics in $\hat{\gamma}_i \circ \psi_i - \gamma$ over each $[t_j, t_{j+3}]$, where $j = 0, 3, 6, \ldots, n-3$. The asymptotics from Th. 1 (with all asymptotic constants independent from n) holding for each Bézier cubic curve $\hat{\gamma}_i$ extends to piecewise Bézier cubic curve $\hat{\gamma}$ and ψ. Indeed the latter follows upon recalling that $\gamma, \hat{\gamma} \circ \psi \in C^0$ (as $\hat{\gamma} \in C^0$) over a compact set $[0,T]$ and $\|\hat{\gamma} \circ \psi - \gamma\|_\infty = \sup_{t \in [0,T]} \|\hat{\gamma}(\psi(t)) - \gamma(t)\| = \max_{t \in [0,T]} \|\hat{\gamma}(\psi(t)) - \gamma(t)\| = \max_{l=0,3,6,\ldots,n-3}\{\max_{t \in [t_l, t_{l+3}]} \|\hat{\gamma}_l(\psi_l(t)) - \gamma(t)\|\}$.

ICCS Camera Ready Version 2026
To cite this paper please use the final published version:
DOI: 10.1007/978-3-032-29909-3_25

5 Main Result

In this section we prove the main result of this work establishing the convergence rate of piecewise Bézier cubic curve $\hat{\gamma}$ in approximating the interpolant γ, for $n \to \infty$ (i.e. for reduced data $Q_n = \{q_i\}_{i=0}^n$ getting denser).

Theorem 1. *Let γ be a $C^2([0,T])$ curve in $\mathbb{E}^m$ sampled admissibly* (1). *For each Bézier cubic curve $\hat{\gamma}_i : [0,1] \to \mathbb{E}^m$ from* (4) *and mapping $\psi_i : I_i = [t_i, t_{i+3}] \to [0,1]$ (see* (5)*) a linear convergence rate in trajectory estimation follows, i.e.:*

$$\hat{\gamma}_i \circ \psi_i - \gamma = O(\delta_n). \tag{7}$$

In particular, if $\mathcal{T}_n$ is also a uniform sampling (here $\delta_n = T/n$ as $K_l = K_u = T$) an acceleration in (7) *occurs resulting in a quadratic convergence order:*

$$\hat{\gamma}_i \circ \psi_i - \gamma = O(\delta_n^2). \tag{8}$$

Consequently, for $\mathcal{T}_n$ more-or-less uniform (2) *the term δ_n in* (7) *and in* (8) *can be optionally replaced by $1/n$. Finally, for each ε-uniform sampling* (3) *the order from* (7) *increases from a linear to a quadratic one, according to the following formula (for $\varepsilon > 0$):*

$$\hat{\gamma}_i \circ \psi_i - \gamma = O(\frac{1}{n^{\min\{2,1+\varepsilon\}}}). \tag{9}$$

Proof. Combining interpolation conditions $\gamma(t_i) = \hat{\gamma}_i(0) = q_i$ and $\gamma(t_{i+3}) = \hat{\gamma}_i(1) = q_{i+3}$ with $\psi_i(t_i) = 0$, $\psi_i(t_{i+3}) = 1$ and $\gamma \in C^2$ together with Hadamard's Lemma (see [34]) applied to $\hat{\Theta}(t) = (\hat{\gamma}_i \circ \psi_i)(t) - \gamma(t)$ over I_i yields:

$$\hat{\Theta}(t) = (t - t_i)(t - t_{i+3})O((\hat{\gamma}_i \circ \psi_i)''(t) - \ddot{\gamma}(t)). \tag{10}$$

Since $\gamma \in C^2$ and $[0,T]$ is compact we have $\ddot{\gamma} = O(1)$. The latter combined with (6) and chain rule results in (for $t \in I_i$, for $i = 0, 3, 6, \ldots, n-3$):

$$\begin{aligned}\hat{\Theta}(t) &= (t - t_i)(t - t_{i+3})O(\hat{\gamma}_i''(s)(\dot{\psi}_i(t))^2 + \hat{\gamma}_i'(s)\ddot{\psi}(t) - \ddot{\gamma}(t)) \\ &= (t - t_i)(t - t_{i+3})O(\hat{\gamma}_i''(s)(\frac{1}{t_{i+3} - t_i})^2 - \ddot{\gamma}(t)) \\ &= (t - t_i)(t - t_{i+3})(O(1) + (\frac{1}{t_{i+3} - t_i})^2 \cdot \hat{\gamma}_i''(s)).\end{aligned} \tag{11}$$

By (4) the second derivative $\hat{\gamma}_i''(s)$ reads as (for $s \in [0,1]$):

$$\hat{\gamma}_i''(s) = 6(1-s)(q_{i+2} - 2q_{i+1} + q_i) + 6s(q_{i+3} - 2q_{i+2} + q_{i+1}). \tag{12}$$

One can reformulate both components from (12) into (for $k = i, i+1$)

$$q_{k+2} - 2q_{k+1} + q_k = (q_{k+2} - q_{k+1}) - (q_{k+1} - q_k). \tag{13}$$

ICCS Camera Ready Version 2026
To cite this paper please use the final published version:
DOI: 10.1007/978-3-032-29909-3_25

Recalling now that all control points $\mathcal{Q}_i = \{q_i, q_{i+1}, q_{i+2}, q_{i+3}\}$ are also interpolation points of γ with $\gamma(t_{i+j}) = q_{i+j}$, (for $j = 0, 1, 2, 3$), Taylor's expansion applied to $\gamma \in C^2$ yields:

$$\begin{aligned} q_{k+1} - q_k &= \gamma(t_{k+1}) - \gamma(t_k) = \gamma(t_k) + \dot{\gamma}(t_k)(t_{k+1} - t_k) + O((t_{k+1} - t_k)^2) - \gamma(t_k) \\ &= \dot{\gamma}(t_k)(t_{k+1} - t_k) + O((t_{k+1} - t_k)^2). \end{aligned} \tag{14}$$

Consequently as $\gamma \in C^2$ we have $\dot{\gamma}(t_{k+1}) = \dot{\gamma}(t_k) + O(t_{k+1} - t_k)$ (for $k = i, i+1$) and thus upon coupling (13) with (14) we arrive at:

$$\begin{aligned} \lambda_i &= q_{i+2} - 2q_{i+1} + q_i \\ &= \dot{\gamma}(t_{i+1})(t_{i+2} - t_{i+1}) + O((t_{i+2} - t_{i+1})^2) - \dot{\gamma}(t_i)(t_{i+1} - t_i) + O((t_{i+1} - t_i)^2) \\ &= \dot{\gamma}(t_i)[(t_{i+2} - t_{i+1}) - (t_{i+1} - t_i)] \\ &\quad + O((t_{i+1} - t_i)^2) + O((t_{i+2} - t_{i+1})^2) + O((t_{i+1} - t_i)(t_{i+2} - t_{i+1})) \end{aligned} \tag{15}$$

and similarly

$$\begin{aligned} \lambda_{i+1} &= q_{i+3} - 2q_{i+2} + q_{i+1} \\ &= \dot{\gamma}(t_{i+2})(t_{i+3} - t_{i+2}) + O((t_{i+3} - t_{i+2})^2) - \dot{\gamma}(t_{i+1})(t_{i+2} - t_{i+1}) + O((t_{i+2} - t_{i+1})^2) \\ &= \dot{\gamma}(t_{i+1})[(t_{i+3} - t_{i+2}) - (t_{i+2} - t_{i+1})] \\ &\quad + O((t_{i+2} - t_{i+1})^2) + O((t_{i+3} - t_{i+2})^2) + O((t_{i+2} - t_{i+1})(t_{i+3} - t_{i+2})). \end{aligned} \tag{16}$$

Combining now (15) and (16) with (12) and taking into account that both expressions $6(1-s) = O(1)$ and $6s = O(1)$ (as $s \in [0, 1]$) one obtains:

$$\begin{aligned} \frac{1}{(t_{i+3} - t_i)^2}\gamma_i''(s) &= \frac{1}{(t_{i+3} - t_i)^2}[6(1-s)\lambda_i + 6s\lambda_{i+1}] \\ &= \frac{1}{t_{i+3} - t_i}\left[O(1)\frac{1}{t_{i+3} - t_i}\lambda_i + O(1)\frac{1}{t_{i+3} - t_i}\lambda_{i+1}\right]. \end{aligned} \tag{17}$$

By (1), (15), $\dot{\gamma} \in C^1([0, T])$, $0 < (t_{i+1} - t_i)(t_{i+3} - t_i)^{-1} < 1$ and $0 < (t_{i+2} - t_{i+1})(t_{i+3} - t_i)^{-1} < 1$ we arrive at:

$$\begin{aligned} \frac{1}{t_{i+3} - t_i}\lambda_i &= \dot{\gamma}(t_i)\left[\frac{t_{i+2} - t_{i+1}}{t_{i+3} - t_i} - \frac{t_{i+1} - t_i}{t_{i+3} - t_i}\right] \\ &\quad + \frac{t_{i+1} - t_i}{t_{i+3} - t_i}O(t_{i+1} - t_i) + \frac{t_{i+2} - t_{i+1}}{t_{i+3} - t_i}O(t_{i+2} - t_{i+1}) \\ &\quad + \frac{t_{i+1} - t_i}{t_{i+3} - t_i}O(t_{i+2} - t_{i+1}) \\ &= O(1)O(1) + O(1)O(\delta_n) + O(1)O(\delta_n) + O(1)O(\delta_n) = O(1). \end{aligned} \tag{18}$$

Similarly, upon using the inequality $0 < (t_{i+3} - t_{i+2})(t_{i+3} - t_i)^{-1} < 1$ we obtain

$$\frac{1}{t_{i+3} - t_i}\lambda_{i+1} = O(1). \tag{19}$$

ICCS Camera Ready Version 2026
To cite this paper please use the final published version:
DOI: 10.1007/978-3-032-29909-3_25

Hence substituting (18) and (19) into (17) yields

$$\frac{1}{(t_{i+3}-t_i)^2}\gamma_i''(s) = \frac{1}{t_{i+3}-t_i}O(1)$$

and therefore substituting the latter into (11) and upon noting that $0 \leq (t - t_i)(t_{i+3}-t_i)^{-1} \leq 1$ (for $t \in I_i$) results in

$$\begin{aligned}\hat{\Theta}(t) &= (t-t_i)(t-t_{i+3})\left[O(1)+O(1)\frac{1}{t_{i+3}-t_i}\right] = O(\delta_n^2)+\frac{t-t_i}{t_{i+3}-t_i}(t-t_{i+3})O(1) \\ &= O(\delta_n^2)+O(\delta_n)O(1) = O(\delta_n).\end{aligned} \tag{20}$$

Hence the proof of (7) is complete. If additionally, *the admissible sampling* $\mathcal{T}_n$ (see (1)) is also *more-or-less uniform* (see (2)), then as $0 \leq \delta_n \leq K_u/n$ the order $O(\delta_n)$ in (20) can be optionally replaced by the term $O(1/n)$. Furthermore, in case of *uniform sampling* $\mathcal{T}_n$ (where $\delta_n = T/n$ and $K_l = K_u = T$ - see (2)) the linear convergence order from (20) increases to the quadratic one. Indeed, the latter follows upon noting that in (13) the expression $(t_{k+2}-t_{k+1})-(t_{k+1}-t_k) = \delta_n - \delta_n = 0$ (for $k = i, i+1$) resulting in (see also (15) and (16))

$$\frac{1}{(t_{i+3}-t_i)^2}\lambda_i = O(1), \quad \frac{1}{(t_{i+3}-t_i)^2}\lambda_{i+1} = O(1).$$

Coupling the latter with (17) yields

$$\begin{aligned}\frac{1}{(t_{i+3}-t_i)^2}\gamma_i''(s) &= \frac{1}{(t_{i+3}-t_i)^2}[6(1-s)\lambda_i+6s\lambda_{i+1}] \\ &= \left[O(1)\frac{1}{(t_{i+3}-t_i)^2}\lambda_i+O(1)\frac{1}{(t_{i+3}-t_i)^2}\lambda_{i+1}\right] = O(1).\end{aligned} \tag{21}$$

Finally, substituting (21) into (11) leads to (as $\ddot{\gamma} \in C^0([0,T])$ and $t - t_i = O(\delta_n)$ and $t - t_{i+3} = O(\delta_n)$, for $t \in I_i = [t_i, t_{i+3}]$):

$$\begin{aligned}\hat{\Theta}(t) &= (t-t_i)(t-t_{i+3})O(\hat{\gamma}_i''(s)(\frac{1}{t_{i+3}-t_i})^2 - \ddot{\gamma}(t)) \\ &= (t-t_i)(t-t_{i+3})(O(1)+O(1)) = O(\delta_n^2) = O(\frac{1}{n^2}).\end{aligned} \tag{22}$$

Consequently, by (22) as $\delta_n = T/n$ the asymptotics from (8) is justified.

Finally, for arbitrary ε*-uniform sampling* $\mathcal{T}_n$ (clearly (3) implies (2) and thus $0 \leq t_{i+1} - t_i \leq \delta_n \leq K/n$) the second order Taylor expansion of $\phi \in C^2$ at point $x_i = (iT)/n$ yields:

$$\begin{aligned} t_{i+2} &= \phi(\frac{(i+2)T}{n}) + O(\frac{1}{n^{1+\varepsilon}}) = \phi(\frac{iT}{n}) + \dot{\phi}(\frac{iT}{n})\frac{2T}{n} + O(\frac{1}{n^2}), +O(\frac{1}{n^{1+\varepsilon}}), \\ t_{i+1} &= \phi(\frac{(i+1)T}{n}) + O(\frac{1}{n^{1+\varepsilon}}) = \phi(\frac{iT}{n}) + \dot{\phi}(\frac{iT}{n})\frac{T}{n} + O(\frac{1}{n^2}) + O(\frac{1}{n^{1+\varepsilon}}).\end{aligned} \tag{23}$$

ICCS Camera Ready Version 2026
To cite this paper please use the final published version:
DOI: 10.1007/978-3-032-29909-3_25

Hence by (23) the expression $(t_{i+2}-t_{i+1})-(t_{i+1}-t_i)$

$$= \left(\dot{\phi}(\frac{iT}{n})\frac{T}{n}+O(\frac{1}{n^2})+O(\frac{1}{n^{1+\varepsilon}})\right)-\left(\dot{\phi}(\frac{iT}{n})\frac{T}{n}+O(\frac{1}{n^2})+O(\frac{1}{n^{1+\varepsilon}})\right)$$
$$= O(\frac{1}{n^2})+O(\frac{1}{n^{1+\varepsilon}})=O(\frac{1}{n^{\min\{2,1+\varepsilon\}}}). \tag{24}$$

Similarly Taylor expansion applied to ϕ at $x_{i+1}=(i+1)T/n$ yields

$$(t_{i+3}-t_{i+2})-(t_{i+2}-t_{i+1})=O(\frac{1}{n^{\min\{2,1+\varepsilon\}}}). \tag{25}$$

Combining now (15) with (24) (as $\gamma\in C^1$) results in

$$\lambda_i=\dot{\gamma}(t_i)[(t_{i+2}-t_{i+1})-(t_{i+1}-t_i)]+O(\frac{1}{n^2})=O(1)O(\frac{1}{n^{\min\{2,1+\varepsilon\}}})+O(\frac{1}{n^2})$$
$$=O(\frac{1}{n^{\min\{2,1+\varepsilon\}}}). \tag{26}$$

Analogously by (16) and (25) we arrive at

$$\lambda_{i+1}=O(\frac{1}{n^{\min\{2,1+\varepsilon\}}}). \tag{27}$$

Coupling together both (26) and (27) with (12) and (17) renders

$$\hat{\gamma}_i''(s)=O(1)O(\frac{1}{n^{\min\{2,1+\varepsilon\}}})+O(1)O(\frac{1}{n^{\min\{2,1+\varepsilon\}}})=O(\frac{1}{n^{\min\{2,1+\varepsilon\}}}).$$

Consequently substituting the latter into (11) yields (over $I_i=[t_i,t_{i+3}]$)

$$\hat{\Theta}(t)=(t-t_i)(t-t_{i+3})O(1)+\frac{(t-t_i)(t-t_{i+3})}{(t_{i+3}-t_i)(t_{i+3}-t_i)}\cdot\hat{\gamma}_i''(s)$$
$$=O(\frac{1}{n^2})+O(1)O(\frac{1}{n^{\min\{2,1+\varepsilon\}}})=O(\frac{1}{n^{\min\{2,1+\varepsilon\}}}).$$

The proof of (9) is therefore complete.

□

Note that Th. 1 establishes at least a linear order (in terms of δ_n) of γ estimation (sampled *admissibly* (1)) by a piecewise Bézier cubic curve $\hat{\gamma}$. The latter extends to the subfamily of *more-or-less uniform* samplings (2) for which equivalent linear rate in $\hat{\gamma}\circ\psi-\gamma=O(1/n)$ holds. Extra acceleration for *uniform* sampling $\mathcal{T}_n$ (a special case of (2)) yields at least a quadratic rate in $\hat{\gamma}\circ\psi-\gamma=O(1/n^2)$. Finally, if γ is sampled *ε-uniformly* then for $0<\varepsilon\leq 1$ a linear convergence rate in $\hat{\gamma}\circ\psi-\gamma$ accelerates to at least order $1+\varepsilon$. On the other hand, the inequality $\varepsilon>1$ yields at least a constant quadratic rate in $\hat{\gamma}\circ\psi-\gamma=O(1/n^2)$. The latter coincides with the uniform sampling case, indicating that $\varepsilon>1$ represents a small negligible distortion of uniform knots' distribution $t_i=iT/n$ once the asymptotics of $\hat{\gamma}\circ\psi-\gamma$ is examined.

ICCS Camera Ready Version 2026
To cite this paper please use the final published version:
DOI: 10.1007/978-3-032-29909-3_25

We prove now *the sharpness* of the asymptotics from Th. 1. In doing so, by Def. 4 and Def. 5 it suffices to justify the latter for a special sampling $\mathcal{T}_n^s$ and some curve $\gamma^s \in C^2$ with $(\hat{\gamma}_i \circ \psi_i - \gamma^s)(t)$ calculated at a certain point $t^* \in [0, T]$. Note that without loss of generality, the domain $[0, T]$ can be freely shifted.

Example 1. Let C^∞ curve $\gamma_l(t) = (t, 0) \in \mathbb{E}^2$ be sampled ε-uniformly (3) as:

$$t_i = \frac{i}{n} + \frac{(-1)^{i+1}}{3n^{1+\varepsilon}}. \tag{28}$$

We additionally admit $\varepsilon = 0$ as then more-or-less uniformity (2) in (28) still prevails. Such extension permits verification of (7) and (9) with a unified argument valid for all $\varepsilon \geq 0$. Consider now the first subinterval $I_0 = [t_0, t_3]$ with

$$\mathcal{T}_n^{0,3} = \{t_0, t_1, t_2, t_3\} = \{\frac{-1}{3n^{1+\varepsilon}}, \frac{1}{n} + \frac{1}{3n^{1+\varepsilon}}, \frac{2}{n} - \frac{1}{3n^{1+\varepsilon}}, \frac{3}{n} + \frac{1}{3n^{1+\varepsilon}}\}.$$

The first four control points $\mathcal{Q}_0 = \{\gamma_l(t_0), \gamma_l(t_1), \gamma_l(t_2), \gamma_l(t_3)\}$ yield $\mathcal{Q}_0^1$ (with q_i first coordinates listed) equal to $\mathcal{T}_n^{0,3}$.

Furthermore, by (5) the mapping $\psi_0(t) = \frac{3tn^{\varepsilon+1}+1}{9n^\varepsilon+2}$ evaluated at $t^* = \frac{1}{3}(t_1 - t_0) = \frac{1}{3}\left(\frac{1}{n} + \frac{2}{3n^{1+\varepsilon}}\right) \in I_0$ upon simplification yields:

$$\psi_0(t^*) = \frac{3n^\varepsilon + 5}{27n^\varepsilon + 6}. \tag{29}$$

By (4), the Bézier cubic curve $\hat{\gamma}_0 = (\hat{\gamma}_0^1, 0) : [t_0, t_3] \to \mathbb{E}^2$ upon resorting to Mathematica's *Expand* and *Simplify* reformulates into (for $s \in [0,1]$):

$$\hat{\gamma}_0(s) = \left(\frac{8}{3}n^{-1-\varepsilon}s^3 - 4n^{-1-\varepsilon}s^2 + (2n^{-1-\varepsilon} + \frac{3}{n})s - \frac{1}{3}n^{-1-\varepsilon}, 0\right). \tag{30}$$

Hence again *Mathematica* symbolic computation (by (29) and (30)) yields

$$\kappa = \hat{\gamma}_0(\psi_0(t^*)) - \gamma_l(t^*) = \left(\frac{4n^{-1-\varepsilon}(3n^\varepsilon + 5)(21n^\varepsilon - 4)(24n^\varepsilon + 1)}{81(9n^\varepsilon + 2)^3}, 0\right). \tag{31}$$

Consequently upon some arithmetic simplification (as $\varepsilon \geq 0$) we have:

$$\kappa = \left(\frac{4}{81}\frac{1}{n^{1+\varepsilon}}\frac{n^{3\varepsilon}(O(1) + O(1) + O(1))}{n^{3\varepsilon}(729 + O(n^{-\varepsilon}))}, 0\right) = (O(\frac{1}{n^{1+\varepsilon}})\frac{1}{1 + O(n^{-\varepsilon})}, 0). \tag{32}$$

Using now geometric series expansion $\frac{1}{1+O(n^{-\varepsilon})} = 1 + O(n^{-\varepsilon})$ results in $\|\kappa\| = O(\frac{1}{n^{1+\varepsilon}})$. The sharpness of (7) (for $\varepsilon = 0$) and (9) (for $0 < \varepsilon \leq 1$) is therefore justified analytically. Here as $\gamma_l'' = 0$ the second quadratic term $(t - t_i)(t - t_{i+3})\gamma_l''$ from (10) does not control the accelerated asymptotics $O(1/n^{1+\varepsilon})$ (once $\varepsilon > 1$). In fact for γ_l the order $O(\frac{1}{n^{1+\varepsilon}})$ holds for all $\varepsilon \geq 0$. To verify the sharpness of quadratic order in (9) for $\varepsilon > 1$ some curve with $\gamma'' \neq 0$ should be considered. E.g. the symbolic computations for $\gamma_q(t) = (t, t^2)$ with $\mathcal{T}_n^{0,3}$ and $\bar{t} = (t_1 - t_0)/3$

ICCS Camera Ready Version 2026
To cite this paper please use the final published version:
DOI: 10.1007/978-3-032-29909-3_25

yield $(\hat{\gamma}\circ\psi)(\bar{t})-\gamma_q(\bar{t})=\frac{C}{n^2}+O(1/n^{\beta})$, where $C\neq 0$ and $\beta>2$. Similarly, for uniform sampling (with $\delta_n=T/n$) the term $\hat{\gamma}\circ\psi-\gamma_l=0$ enters the machine error with no asymptotics computable. Again different curve than γ_l needs to be selected to justify analytically the sharpness of (8). Indeed, taking e.g. $t_0=0$, $t_1=\delta_n$, $t_2=2\delta_n$, $t_3=3\delta_n$ and $\bar{t}=\delta_n/3$ for γ_q (with $q_i=\gamma_q(t_i)$, for $i=0,1,2,3$) leads to $(\hat{\gamma}\circ\psi)(\bar{t})-\gamma_q(\bar{t})=(0,\frac{8}{27}\delta_n^2)$. We omit full computations for both uniform and $\varepsilon>1$ cases due to page limitation. They are similar to the case $0\leq\varepsilon\leq 1$.

6 Experiments

We numerically verify now the asymptotics from Th. 1. All tests are performed in *Mathematica 12.0* and use two types of *ε-uniform samplings* (here $T=1$):

$$t_i=\begin{cases}\frac{i}{n}+\frac{1}{2n^{1+\varepsilon}}, & \text{for } i=4k+1;\\ \frac{i}{n}-\frac{1}{2n^{1+\varepsilon}}, & \text{for } i=4k+3;\\ \frac{i}{n}, & \text{for } i \text{ even};\end{cases} \tag{33}$$

with $K_l=(1/2)$ and $K_u=(3/2)$ from (2) and

$$t_i=\frac{i}{n}+\frac{(-1)^{i+1}}{3n^{1+\varepsilon}}, \tag{34}$$

with $K_l=(1/2)$ and $K_u=(5/3)$ from (2). For (33) and (34) we admit $\varepsilon=0$.

From the set of absolute errors $E_n=\max_{t\in[0,T]}\|(\hat{\gamma}\circ\psi)(t)-\gamma(t)\|$ (see also (4) and (6)) the estimate $\bar{\alpha}\approx\alpha$ from $O(1/n^{\alpha})$ is computed upon applying a linear regression to the pairs of points $\{(\log(n),-\log(E_n))\}_{n=n_{min}}^{n_{max}}$, with $n=3l$ for $l\in\mathbb{N}$. Note that on one hand n_{min} cannot be too small due to the asymptotical character of Th. 1. On the other hand n_{max} should not be too big as the respective errors in trajectory estimation enter the machine error level. The adjustment of concrete values of n_{min} and n_{max} follows upon testing on each specific sampling $\mathcal{T}_n$ and curve γ. Here we set $n_{min}=60$ and $n_{max}=120$.

Example 2. Consider *a regular planar epitrochoid* $\gamma_{ep}:[0,1]\to\mathbb{E}^2$,

$$\gamma_{ep}(t)=(4\cos(t)-0.15\cos(4\pi t),4\sin(t)-0.15\sin(4\pi t)). \tag{35}$$

Fig. 1(a) (or Fig. 1(b)) contains the plots of γ_{ep} sampled (here $n=18$) according to either (33) (or (34)). The respective estimates $\bar{\alpha}(\varepsilon)\approx\alpha(\varepsilon)$ are computed for various $\varepsilon\in\Omega_{\varepsilon}=\{0,0.1,0.3,0.5,0.7,0.9,1.0,2.0\}$. The numerical results reported in Table 1 confirm the asymptotics from (7) and (9) for $\varepsilon\in\Omega_{\varepsilon}$. The sharpness is here numerically verified in affirmative for $\varepsilon=0.0,0.1,0.3,0.9,1.0,2.0$. The case of $\varepsilon=0.7$ yields a slightly faster convergence order still consistent with (9). For *uniform sampling* the estimate $\bar{\alpha}=1.993$ confirms the sharpness of (8).

Example 3. Let *a cissoid of Diocles curve* $\gamma_{cd}:[0,1]\to\mathbb{E}^2$ be defined as:

$$\gamma_{cd}(t)=\left(2\sin^2(t),2\sin^2(t)\tan(t)\right). \tag{36}$$

ICCS Camera Ready Version 2026
To cite this paper please use the final published version:
DOI: 10.1007/978-3-032-29909-3_25

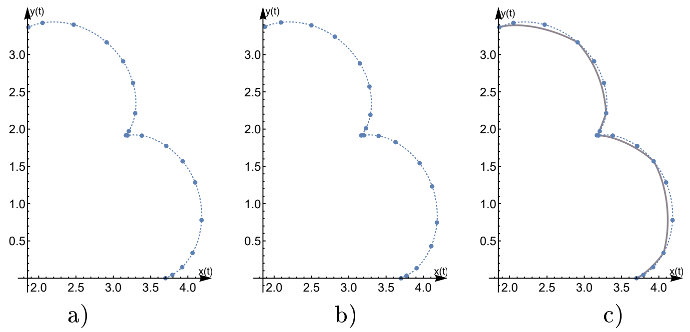

Fig. 1. *An epitrochoid* γ_{ep} (35) sampled along (dotted): a) (33) with $\varepsilon = 0.3$ or b) (34) with $\varepsilon = 0.5$ and c) fitted by $\hat{\gamma}$ with (33) and $\varepsilon = 0.3$ for $n = 18$.

Table 1. Computed $\bar{\alpha}(\varepsilon) \approx \alpha(\varepsilon)$ from (7) and (9) for γ_{ep} in (35) and $\varepsilon \in \Omega_\varepsilon$.

ε	0.0	0.1	0.3	0.5	0.7	0.9	1.0	2.0
$\bar{\alpha}(\varepsilon)$ for (33)	1.020	1.133	1.400	1.709	1.902	1.989	2.002	1.993
$\bar{\alpha}(\varepsilon)$ for (34)	1.090	1.231	1.592	1.906	1.994	1.993	1.993	1.993
$\alpha(\varepsilon)$ in Th. 1	1.0	1.1	1.3	1.5	1.7	1.9	2	2

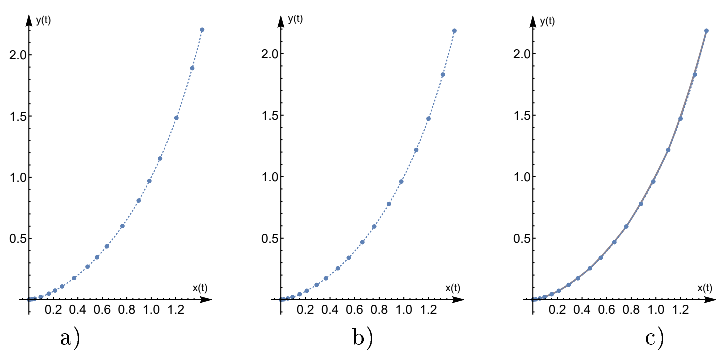

Fig. 2. *A cissoid of Diocles* γ_{cd} (36) sampled along (dotted): a) (33) with $\varepsilon = 0.3$ or b) (34) with $\varepsilon = 0.7$ and c) fitted by $\hat{\gamma}$ with (34) and $\varepsilon = 0.7$ for $n = 18$.

ICCS Camera Ready Version 2026
To cite this paper please use the final published version:
DOI: 10.1007/978-3-032-29909-3_25

Fig. 2(a) or Fig. 2(b) illustrate the trajectories of γ_{cd} sampled according to either (33) or (34), with $n = 18$. As previously, a linear regression estimating $\bar{\alpha}(\varepsilon) \approx \alpha(\varepsilon)$ is used for various $\varepsilon \in \Omega_\varepsilon$. Table 2 enlists numerically computed estimates $\bar{\alpha}(\varepsilon) \approx \alpha(\varepsilon)$ for $\varepsilon \in \Omega_\varepsilon$ and for either samplings (33) or (34). Visibly for $\varepsilon = 0, 0.1, 0.3, 0.5, 0.7, 0.9, 1.0, 2.0$ the numerical results confirm the sharpness of the asymptotics determined by (7) and (9). The *uniform sampling* for γ_{cd} results in estimate $\bar{\alpha} = 1.928$ verifying in affirmative the sharpness of (8).

Table 2. Computed $\bar{\alpha}(\varepsilon) \approx \alpha(\varepsilon)$ in (7) and (9) for γ_{cd} from (36) and various $\varepsilon \in \Omega_\varepsilon$.

ε	0.0	0.1	0.3	0.5	0.7	0.9	1	2
$\bar{\alpha}(\varepsilon)$ for (33)	0.958	1.058	1.245	1.478	1.682	1.810	1.840	1.928
$\bar{\alpha}(\varepsilon)$ for (34)	1.019	1.139	1.401	1.663	1.854	1.923	1.930	1.928
$\alpha(\varepsilon)$ in Th. 1	1.0	1.1	1.3	1.5	1.7	1.9	2	2

Finally, *a conical spiral* γ_{cs} in $\mathbb{E}^3$ is tested.

Example 4. Let *a conical spiral* $\gamma_{cs} : [0, 1] \to \mathbb{E}^3$ be defined as follows:

$$\gamma_{cs}(t) = (2\sin(0.5\pi t)\cos(2\pi t), 2\sin(0.5\pi t)\sin(2\pi t), 2\cos(0.5\pi t)). \qquad (37)$$

Fig. 3(a) or Fig. 3(b) contain the plots of γ_{cs} sampled ε-uniformly along either (33) or (34) (here $n = 18$).

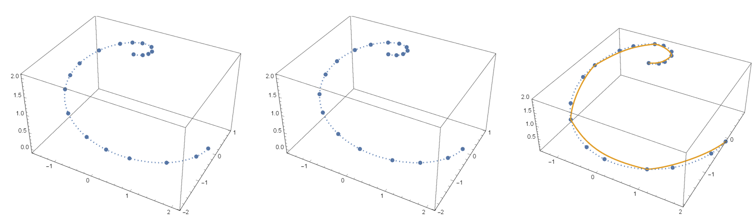

a) b) c)

Fig. 3. *A conical spiral* γ_{cs} (37) sampled along (dotted): a) (33) with $\varepsilon = 0.3$ or b) (34) with $\varepsilon = 0.7$ and c) fitted by $\hat{\gamma}$ with (34) and $\varepsilon = 0.3$ for $n = 18$.

In order to compute $\bar{\alpha}(\varepsilon) \approx \alpha(\varepsilon)$ various $\varepsilon \in \Omega_\varepsilon$ are used. Table 3 enlists numerically computed estimates $\bar{\alpha}(\varepsilon) \approx \alpha(\varepsilon)$ for $\varepsilon \in \Omega_\varepsilon$ and for either samplings (33) or (34). Visibly for $\varepsilon = 0, 0.1, 0.3, 0.9, 1.0, 2.0$ the numerical results confirm the sharpness of the asymptotics determined by (7) and (9). The remaining cases of $\varepsilon = 0.5, 0.7$ are consistent with Th. 1 which states that the respective convergence order should be at least 1.5 and 1.7. The *uniform sampling* for γ_{cs} results in numerical estimate $\bar{\alpha}$=1.997 verifying in affirmative the sharpness of (8).

ICCS Camera Ready Version 2026
To cite this paper please use the final published version:
DOI: 10.1007/978-3-032-29909-3_25

Table 3. Computed $\bar{\alpha}(\varepsilon) \approx \alpha(\varepsilon)$ from (7) and (9) for γ_{cs} in (37) and various $\varepsilon \in \Omega_\varepsilon$.

ε	0.0	0.1	0.3	0.5	0.7	0.9	1.0	2.0
$\bar{\alpha}(\varepsilon)$ for (33)	1.010	1.113	1.359	1.674	1.927	1.990	1.993	1.997
$\bar{\alpha}(\varepsilon)$ for (34)	1.060	1.186	1.536	1.987	1.997	1.997	1.997	1.997
$\alpha(\varepsilon)$ in Th. 1	1.0	1.1	1.3	1.5	1.7	1.9	2.0	2.0

7 Conclusion

This work investigates the asymptotics in estimating the curve $\gamma \in C^2$ in $\mathbb{E}^m$ by a piecewise Bézier cubic curve $\hat{\gamma}$ (see Section 3). Here the interpolant $\hat{\gamma}$ fits less than half of reduced data Q_n^p (i.e. only $Q_n^p \subset Q_n$). The remaining points $Q_n \setminus Q_n^p$ serve merely as control points. In exchange for such "sparser interpolation", the fitting curve $\hat{\gamma}$ preserves all local geometrical features of Bézier cubic curves (see Section 3). Consequently, the curve $\hat{\gamma}$ can satisfy both $\hat{\gamma} \approx \gamma$ (once $n \to \infty$) and specific geometrical constraints a priori imposed on $\hat{\gamma}$. The *main theoretical contribution of this work* established in Th. 1 (see Section 5) proves *linear, quadratic or* $\min\{2, 1+\varepsilon\}$ sharp convergence rates in $\hat{\gamma} \approx \gamma$ once γ is sampled *admissibly/more-or-less uniformly, uniformly or ε-uniformly.* In Section 6, the outcomes of numerical tests conducted on 2D and 3D curves confirm in affirmative the asymptotics (and sharpness) from Th. 1. *Possible applications* of this work include geometrical modelling and approximation. In particular, in dynamical active tracking the positions Q_n of tracked object usually arrive in batches (e.g. $\mathcal{Q}_i$) at various times (known or unknown). The tracker may opt not to interpolate $\{q_i, q_{i+1}\}$, but rather reaching q_{i+3} and keeping $\hat{\gamma}$ trajectory inside the convex hull spanned by $\mathcal{Q}_i$. Upon reaching q_{i+3} the next batch of information i.e. $\mathcal{Q}_{i+3}$ arrives to initiate the above strategy again. Other applications and/or extensions of this work may refer to boundary modelling or its length estimation for which the smoothness of $\hat{\gamma}$ at junction points Q_n^p is not essential. In contrast, if smoothness constraint imposed at junction points is vital then a possible alternative is to apply B-splines (see e.g. [3, 4, 12, 32, 37]). More related work together with some applications (in *computer graphics and vision, image processing, engineering, trajectory planning and tracking, curve shaping and approximation*) on modelling and/or on fitting reduced sparse or dense data Q_n with various schemes $\hat{\gamma}$ and choices of $\hat{\mathcal{T}}_n$ can be found e.g. in [1, 3, 8–10, 13, 14, 16, 18, 19, 29–33, 35, 37, 38, 40, 41].

References

1. Atkinson, K.: On the order of convergence of natural cubic spline interpolation. SIAM J. Numer. Anal. **5**(1), 89–101 (1968). https://doi.org/10.1137/0705007
2. Beccari, C.V., Casciola, G., Romani, L.: Non-uniform interpolatory curve subdivision with edge parameters built upon compactly supported fundamental splines. BIT Numer. Math. **51**, 781–808 (2011). https://doi.org/10.1007/s10543-011-0328-2

ICCS Camera Ready Version 2026
To cite this paper please use the final published version:
DOI: 10.1007/978-3-032-29909-3_25

3. Bézier, P.E.: Numerical Control: Mathematics and Applications. John Wiley, New York (1972)
4. de Boor, C.: A Practical Guide to Spline. Springer-Verlag, New York Heidelberg Berlin (1985)
5. do Carmo, M.P.: Differential Geometry of Curves and Surfaces, Prentice-Hall, Engelwoods Cliffs, New Jersey (1976)
6. Dubuc, S.: Interpolation through an iterative scheme. J. Math. Anal. Appl. **114**(1), 185–204 (1986). https://doi.org/10.1016/0022-247X(86)90077-6
7. Dyn, N., Floater, M.S., Harmann, K.: Four-point curve subdivision based on iterated chordal and centripetal parameterization. Comput. Aided Geom. Design **26**(3), 279–286 (2009). https://doi.org/10.1016/j.cagd.2008.09.006
8. Epstein, M.P.: On the influence of parameterization in parametric interpolation. SIAM J. Numer. Anal. **13**, 261–268 (1976). https://doi.org/10.1137/0713025
9. Farin, G.: Curves and Surfaces for Computer Aided Geometrical Design. Academic Press, San Diego (1993)
10. Floater, M.S.: Chordal cubic spline interpolation is fourth order accurate. IMA J. Numer. Anal. **26**, 25–33 (2006). https://doi.org/10.1093/imanum/dri022
11. Floater, M.S., Surazhsky, T.: Parameterization for curve interpolation. Stud. Comput. Math. **12**, 39–54 (2006). https://doi.org/10.1016/S1570-579X(06)80004-2
12. Haron, H., Rehman, A., Adi, D.I.S., Lim, S.P., Saba, T.: Parameterization method on B-spline curve. Math. Probl. Eng. **2012**(1), 1–22 (2012). https://doi.org/10.1155/2012/640472
13. Janik, M., Kozera, R., Kozioł, P.: Reduced data for curve modeling - applications in graphics, computer vision and physics. Adv. Sci. Tech. **7**(18), 28–35 (2013). https://doi.org/10.5604/20804075.1049599
14. Juhász, J., Hoffmann, M.: On parameterization of interpolating curves. J. Comput. Appl. Math. **216**(2), 413–424 (2008). https://doi.org/10.1016/j.cam.2007.05.019
15. Klingenberg, W.: A Course in Differential Geometry. Springer-Verlag, Berlin Heidelberg (1978)
16. Kocić, Lj.M., Simoncelli, A.C., Della Vecchia, B.: Blending parameterization of polynomial and spline interpolants. Facta Univ. (NIS) Ser. Math. Inform. **5**, 95–107 (1990)
17. Kozera, R.: Curve modeling via interpolation based on multidimensional reduced data. Stud. Inform. **25**(4B-61), 1–140 (2004)
18. Kozera, R., Noakes, L.: C^1 Interpolation with cumulative chord cubics. Fund. Inform. **61**(3-4), 285–301 (2004). https://doi.org/10.3233/FUN-2004-613-406
19. Kozera, R., Noakes, L.: Piecewise-quadratics and exponential parameterization for reduced data. Appl. Math. Comput. **221**, 620–638 (2013). https://doi.org/10.1016/j.amc.2013.06.060
20. Kozera, R., Noakes, L., Wilkołazka M.: Parameterizations and Lagrange cubics for fitting multidimensional data. In: Krzhizhanovskaya V. et al. (eds) Computational Science - ICCS 2020, LNCS, vol 12138, pp. 124–140. Cham, Springer (2020). https://doi.org/10.1007/978-3-030-50417-5_10
21. Kozera R., Noakes, L., Wiliński, A.: Generic case of Leap-Frog Algorithm for optimal knots selection in fitting degenerate data. In: Paszyński M. et al. (eds) Computational Science - ICCS 2021, LNCS, vol 12745, pp. 337–350. Cham, Springer (2021). https://doi.org/10.1007/978-3-030-77970-2_26
22. Kozera R., Noakes, L.: Non-generic case of Leap-Frog Algorithm for optimal knots selection in fitting degenerate data. In: Groen J. et al. (eds) Computational Science - ICCS 2022, LNCS, vol 13352, pp. 341–454. Cham, Springer (2022). https://doi.org/10.1007/978-3-031-08757-8_29

23. Kozera, R., Noakes, L.: Optimal knots selection in fitting degenerate data. In: Mikyška J. et al. (eds) Computational Science - ICCS 2023, LNCS, vol 10475, pp. 439–453. Cham, Springer (2023). https://doi.org/10.1007/978-3-031-36024-4_34
24. Kozera, R., Noakes, L. Wilkołazka: Asymptotics in curve estimation by modified cubic spline and exponential parameterization. In: Paszyński M. et al. (eds) Computational Science - ICCS 2025, LNCS, vol 15908, pp. 316–331. Cham, Springer (2025). https://doi.org/10.1007/978-3-031-97557-8_23
25. Kozera, R., Wilkołazka, M.: A note on modified Hermite interpolation. Math. Comput. Sci. **14**, 223–239 (2020). https://doi.org/10.1007/s11786-019-00434-3
26. Kozera, R., Noakes, L., Wilkołazka, M.: A modified complete spline interpolation and exponential parameterization. In: Computer information systems and industrial management - CISIM 2015, LNCS, vol 9339, pp. 98–110, Springer-Verlag (2015). https://doi.org/10.1007/978-3-319-24369-6_8
27. Kozera, R., Wilkołazka, M.: Convergence order in trajectory estimation by piecewise-cubics and exponential parameterization. Math. Model. Anal. **24**(1), 72–94 (2019). https://doi.org/10.3846/mma.2019.006
28. Kuznetsov, E.B., Yakimovich, A.Y.: The best parameterization for parametric interpolation. J. Comput. Appl. Math. **191**(2), 239–245 (2006). https://doi.org/10.1016/j.cam.2005.06.040
29. Kvasov, B.I.: Methods of Shape-Preserving Spline Approximation. World Scientific, Singapore (2000)
30. Lee, E.T.Y.: Choosing nodes in parametric curve interpolation. Comput. Aided Design **21**(6), 363–370 (1989). https://doi.org/10.1016/0010-4485(89)90003-1
31. Lee, E.T.Y.: Corners, cusps, and parameterization: variations on theorem of Epstein. SIAM J. of Numer. Anal. **29**, 553–565 (1992). https://doi.org/10.1137/0729035
32. Lim, C.G.: Universal parameterization method in B-spline curve and surface interpolation. Comput. Aided Geom. Design **16**(5), 407–422 (1999). https://doi.org/10.1016/S0167-8396(99)00010-2
33. Marin, S.P.: An approach to data parameterization in parametric cubic spline interpolation problems. J. Approx. Theory **41**(6), 64–86 (1984). https://doi.org/10.1016/0021-9045(84)90121-7
34. Milnor, J.: Morse Theory, Annals of Mathematics Studies, Princeton University Press (1968)
35. Mørken, K., Scherer, K.: A general framework for high-accuracy parametric interpolation. Math. Comp. **66**(217), 237–260 (1997). https://doi.org/10.1090/S0025-5718-97-00796-5
36. Noakes, L., Kozera, R.: More-or-less uniform samplings and length of curves. Quart. Appl. Math. **61**(3), 475–484 (2003). https://doi.org/10.1090/QAM/1999832
37. Piegl, L. Tiller, W.: The NURBS Book. Springer-Verlag, Berlin Heidelberg (1997)
38. Rababah, A.: High order approximation methods for curves. Comput. Aided Geom. Design **12**, 89–102 (1995).
39. Shalashilin, V.I., Kuznetsov, E.B.: Parametric Continuation and Optimal Parameterization in Applied Mathematics and Mechanics. Kluver Academic Publishers, Dordrecht Boston London (2003)
40. Shamsuddin, S.M.H, Ahmed, M.A.: A hybrid parameterization method for NURBS. In: Proc. 2nd Int. Conf. Computer Graphics, Imaging and Visualization pp. 5–20. IEEE Comp. Soc., Penang Malaysia (2004). https://doi.org/10.1109/CGIV.2004.1323954
41. Williams, J.R., Thwaites, D. J.: Radiotherapy Physics in Practice, Oxford University Press, Oxford (2000)

ICCS Camera Ready Version 2026
To cite this paper please use the final published version:
DOI: 10.1007/978-3-032-29909-3_25